ORIGINAL RESEARCH

Effect of parameter values on fingerprint filtering

Akinyokun O. Charles*[1], Iwasokun B. Gabriel[1], Angaye O. Cleopas[2]

[1]*Department of Computer Science, Federal University of Technology, Akure, Nigeria*
[2]*Department of Computer Science, Niger Delta University, Wilberforce Island, Nigeria*

ABSTRACT

Fingerprint is presently the most significant biometric for human verification and identification. The reason being its highest degree of uniqueness, availability, durability and consistency when compared with other biometrics such as face, nose, iris, ear, palm print and signature. The use of fingerprint in human identity management spans through stages of enrolment, enhancement, feature extraction and pattern matching. The enhancement stage involves ridge segmentation, normalization, orientation estimation, frequency estimation, filtering, binarization and thinning. Filtering is the stage at which all forms of noise and contaminations introduced into the image during enrolment are removed. The removal of noise and contaminations is necessary for accurate feature extraction and pattern matching. In some of the existing fingerprint image filtering algorithms, accurate and appropriate parameter selections are essential for obtaining optimal and satisfactory results. In this research, the existing Gabor filter was modified and the values of some standard parameters were varied. Experimental study on the adequacy of the modified algorithm and its parameter values on fingerprint filtering were investigated on the standard FVC2002 fingerprint database. Comparative analysis of the obtained results with what were obtained from some existing algorithms shows satisfactory and acceptable performances of the modified algorithm.

Key Words: Fingerprint, Image processing, Gabor filter, Minutiae point

1. INTRODUCTION

In different areas of human endeavor, fingerprint has continued to establish its superiority in human verification and identification. The preference for fingerprint over other types of biometrics such as face, nose, iris, palm print, gait, DeoxyriboNucleic Acid (DNA) and signature has been attributed to factors including high degree of uniqueness, availability, universality, reliability and durability.[1–4] These factors have contributed to the development of several Automated Fingerprint Identification System (AFIS) for attendant management, access control, financial transactions, human traffic control and criminal investigation among others.[5] Prominent and es-

sential functionalities of AFIS include fingerprint enrolment, enhancement, feature extraction and pattern recognition and matching.[6] An AFIS relies on a number of live scan devices for the enrolment of fingerprints. These devices are categorized into optical, electrical and ultrasonic sensors.[7–11] Due to the presence of injury, dirt or liquid, image produced by the scanning device often experiences noise or distortion which may ultimately degrade the performance of the system. The solution to this is to provide AFIS with mechanism for image enhancement. The mechanism adopts a serial process of segmentation, normalization, filtering, binarization and thinning for the removal of noise and distortions.[12–14] Segmentation is used as a first step to separate the foreground

---

*Correspondence:** Akinyokun O. Charles; Email: admin@akinyokun.com; Address: Department of Computer Science, Federal University of Technology, Akure, Nigeria.

(regions containing ridges and valleys) from the background (noisy regions). By normalization, the grey-level values of the segmented image are standardized to a uniform level while filtering is ultimately performed as the basis for tuning the normalized image and eliminating all forms of noise-induced ridge deficiencies or overlaps. A noisy fingerprint and its filtered image are shown in Figure 1.
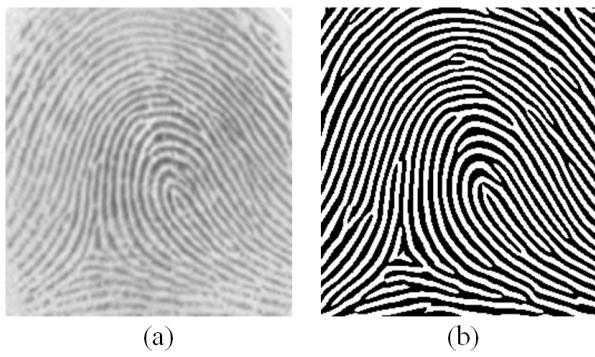

(a)   (b)

Figure 1. (a) Noisy Image, (b) Filtered Image.

There exist several research works on fingerprint filtering. The authors[15–17] proposed improved Gabor Filter (GF) algorithms for fingerprint image filtering. The algorithms preserve fingerprint image ridge structure with enhancement consistency but failed with greatly contaminated and heavily noisy images.

The authors[18] proposed a Short Time Fourier Transform Analysis (STFTA), which is a signal processing technique-based algorithm for fingerprint filtering. Based on probabilistic approach for robust estimation of associated parameters, the algorithm simultaneously estimates all the intrinsic properties of the fingerprints such as the foreground region mask and local ridge orientation and frequency. The performance of the algorithm is heavily dependent on its orientation smoothening algorithm which fails significantly with highly contaminated images. Prajakta *et al.*[19] used a bank of Gabor filters to provide a basis for implementing extremely fast fingerprint identification. The filters merely perform selective filtering of fingerprint images while capturing both local and global details as a compact fixed length Finger Code.

Fingerprint is enhanced by using local ridge orientation-based directional filter.[20] The orientation of the filter is everywhere matched to the ridge orientation and the enhanced image is produced based on thresholding. The major setback to the algorithm is its position-dependent nature which makes it susceptible to ripples across edges. Aarthy *et al.*[21] proposed a 2-stage scheme for filtering low-quality fingerprint image in spatial and frequency domains using Fast Fourier Transform (FFT) algorithm. The algorithm is suitable for

the recovering of corrupted regions in some fingerprints but highly dependent on the radial and angular domains properties which are not obtainable in some images. Josef *et al.*[22] used directional filters and binarization to filter fingerprint local area through adaptive analysis and adjustment of the entire image in the frequency domain. The algorithm is capable of adaptively adjusting the local area of the fingerprint image and is independent of fingerprint physical or sensor characteristic. It however experiences high operational time due to complex computations. In Ref.,[23] a high boost fingerprint enhancement algorithm that is based on Gaussian filter, Mean Squared Error (MSE) and Peak Signal Noise Ratio (PSNR) is proposed. The algorithm exhibits adequacy in the enhancement of Region of Interest (RoI) but experiences complex computations with low convergence rate due mainly to sharp discontinuities between the image edges which results in large magnitude and high spatial frequency components.

Zhang *et al.*[24] presented a space-frequency and quality factor-based fingerprint filtering algorithm. The quality factor is calculated based on the orientation field of the image. The algorithm generates high numbered enhancement artefacts due to restriction of filtering to regions with high noise density and insufficient quality factors. The authors[25] proposed Wiener and anisotropic-based algorithms for fingerprint image filtering. Though the algorithms exhibit improvement over some existing algorithms in terms of speed and accuracy, they are only applicable to enhancement of gray-scale images. Ali *et al.*[26] used a combination of diffusion-coherence and spatial domain 2D-Gabor filters to remove the blocking artefacts in an enhanced fingerprint image. The method significantly filtered the image core region and the plane ridge-valley but requires tedious task for its parameter setting. Aguilar *et al.*[27] used a combination of FFT and Gabor filters for fingerprint enhancement. The combination of the two filters significantly enhanced the high curvature regions of the image but experiences large storage requirements.

With focus on addressing the reported limitations, a modified version of the Gabor filter-based algorithm for fingerprint image filtering is presented in this paper. The experimental study of the effect of varying the values of some standard parameters on fingerprint filtering is also presented. Gabor filter as a fingerprint filtering technique is presented in Section 2 while Section 3 presents the modified fingerprint filtering technique. Sections 4 and 5 present findings from the experimental studies and the conclusions drawn from the research respectively.

2. GABOR FILTERING TECHNIQUE

Gabor filter is a very useful tool in fingerprint image processing, especially for texture analysis, due to its optimal localization properties in both spatial and frequency domain. Several researches on its applications have been carried out. Gabor[28] proposed one dimensional (1-D) Gabor function. Research on 2-D Gabor filters began[29] as a platform for understanding the orientation and spatial properties of neurons in the brains' visual cortex. Further mathematical elaboration of 2-D Gabor function was presented in Ref.[30] Hong et al.[31] used Gabor filter banks to enhance fingerprint images with the assumption that the parallel ridges and valleys possess normal sinusoidal-shaped plane waves common to some noises. The Gabor filter is tuned to the corresponding local orientation and ridge frequency (reciprocal of ridge distance) in order to remove noises and preserve the genuine ridge and valley structures. However, there is inaccuracy in the assumption due to the fact that the signal orthogonal to the local orientation in practice possesses no ideal digital sinusoidal plane wave in some fingerprint images or regions as shown in Figure 2.[15]
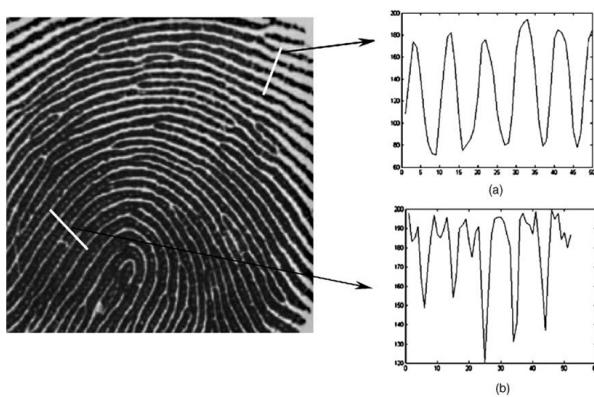

Figure 2. Ridge and valley topography of a fingerprint image. The top-right region can be approximately treated as a sinusoidal plane wave while the bottom-left cannot.

Dhanabal et al.[17] present a fingerprint filtering technique in which the incoming signal in the form of image pixel is convoluted by Gabor filter to define the edge and vale regions of the image. The image's Gabor impulse response, g with real and imaginary components, is given by the product of the harmonic and the Gaussian functions as follows:

$$\mathcal{G} = \mathcal{P} * \yen \tag{1}$$

P is the Gaussian function and $\yen$ is the Fourier Transform. The complex, real and imaginary components are obtained from Equation 2, 3 and 4 respectively.

$$\mathcal{G}(p, q: \mu, \vartheta, \rho, \varphi) = e^{-\frac{(a^2+b^2)}{2\varphi^2}} \times e^{\left(i\left(\frac{2\pi a}{\mu} + \rho\right)\right)} \tag{2}$$

$$\mathcal{G}(p, q: \mu, \vartheta, \rho, \varphi) = e^{-\frac{(a^2+b^2)}{2\varphi^2}} \times \cos\left(i\left(\frac{2\pi a}{\mu} + \rho\right)\right) \tag{3}$$

$$\mathcal{G}(p, q: \mu, \vartheta, \rho, \varphi) = e^{-\frac{(a^2+b^2)}{2\varphi^2}} \times \sin\left(i\left(\frac{2\pi a}{\mu} + \rho\right)\right) \tag{4}$$

$$a = p\cos\theta + q\sin\theta \tag{5}$$

$$b = p\sin\theta + q\cos\theta \tag{6}$$

μ is the wavelength of the sinusoidal factor, ϑq represents the orientation of the Gabor function, ρ denotes the phase offset, and φ denotes the Gaussian envelope.

The general form of even symmetric Gabor filtering is presented in Ref.[16,31,32] as follows:

$$R(x, y, f, \varphi) = \frac{1}{2\pi\sigma_x\sigma_y} e^{-\frac{1}{2}\left(\frac{x_\varphi^2}{\sigma_x^2} + \frac{y_\varphi^2}{\sigma_y^2}\right)} \cos\left(2\pi f x_\varphi\right) \tag{7}$$

$$\begin{bmatrix} x_\varphi \\ y_\varphi \end{bmatrix} = \begin{bmatrix} \cos\varphi & \sin\varphi \\ -\sin\varphi & \cos\varphi \end{bmatrix} \begin{bmatrix} x \\ y \end{bmatrix} \tag{8}$$

φ is the orientation of the filter, f is the frequency of a sinusoidal plane wave, $[x_\varphi, y_\varphi]$ stands for the axis $[x, y]$ along the counter-clockwise rotation φ degrees.

The authors[15] replaced the cosine function $\cos(x, f)$ with a periodic function $F(x, f_1, f_2)$ to obtain an improved Gabor filter that incorporates two sinusoidal functional curves with varying periods f_1 and f_2. $F(x, f_1, f_2)$ which is extended periodically with mathematical function is as follows:

$$F(x, f_1, f_2) = f(x) - \left[\frac{x}{0.5(f_1 + f_2)}\right] * \left(0.5(f_1 + f_2)\right) \tag{9}$$

$$f(x) = \begin{cases} \cos(2\pi x f_1^{-1}), & 0 \le x \le f_1/4 \\ -\cos\left(2\pi\left(x - \frac{f_1}{4} - \frac{f_2}{4}\right)f_1^{-1}\right), & \frac{f_1}{4} < x < \frac{f_1}{4} + \frac{f_2}{2} \\ \cos\left(2\pi\left(x - \frac{f_1}{2} - \frac{f_2}{2}\right)f_1^{-1}\right), & \frac{f_1}{4} + \frac{f_2}{2} \le x \le \frac{f_1}{2} + \frac{f_2}{2} \end{cases} \tag{10}$$

The Gabor filter was specified by modulating the periodic function $F(x; f_1, f_2)$ by a 2-D anisotropic Gaussian function

to produce the function:

$$g(x, y; f_1, f_2, \emptyset) = h_x(x; y; f_1, f_2, \emptyset) = \left[F(x_\emptyset; f_1, f_2) e^{-\frac{x_\emptyset^2}{2\sigma_x^2}} \right] * \left[e^{-\frac{y_\emptyset^2}{2\sigma_y^2}} \right]$$

(11)

A 2-D Gabor function in the inform of a harmonic oscillator composed of a sinusoidal plane wave of a particular frequency and orientation, within a Gaussian envelope over the image domain (r, s) is defined in Ref.[15] as:

$$G(r, s) = e^{-\left(\left(\frac{w^2}{\beta_r^2} \right) - \left(\frac{z^2}{2\beta_s^2} \right) \right)} e^{-(2\pi i (u_0 w + v_0 z))}$$

(12)

$$w = r - r_0$$

(13)

$$z = s - s_0$$

(14)

(r_0, s_0) denotes the location in the image, (u_0, v_0) is the modulation with spatial frequency τ_0 and orientation θ_0 defined by:

$$\tau_o = \sqrt{u_0^2 - v_0^2}$$

(15)

$$\theta_0 = tan^{-1} \frac{v_0}{u_0}$$

(16)

β_r and β_s are the standard deviations of the Gaussian envelope along x and y axes respectively.

The modification of the traditional Gabor filter[15] produced a way of preserving the fingerprint image topography. However, the challenge of inter-medial parameters determination by experience rather than objectivity is a major problem. To address this drawback, this research introduces a robust image pre-processing (segmentation, normalization and ridge frequency estimation) and an optimal parameter selection technique.

3. MODIFIED GABOR FILTERING TECHNIQUE

The existing Gabor filter-based algorithms for fingerprints filtering rely on a number of parameters whose accurate selection is of utmost importance for optimal image contrast enhancement and filtering.[13, 14, 17, 19] The Gabor filter-based algorithm for fingerprint filtering presented in Ref.[16, 31, 32] was modified before use. The modified version, which comprises of stages for ridge segmentation, ridge normalization,

ridge orientation estimation, ridge frequency estimation and image filtering, is conceptualized in Figure 3.
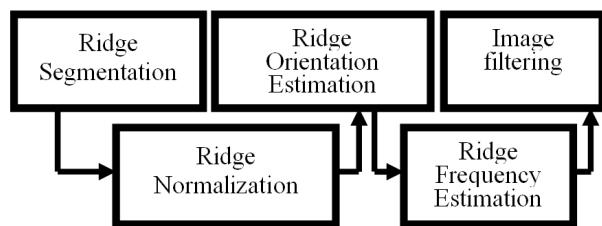

Figure 3. Fingerprint filtering stages

The background regions of a fingerprint image generally exhibit very low grey-scale variance values, whereas the foreground regions have very high variances. Hence, variance thresholding method is used to segment the image. During segmentation, the image is divided into blocks and the grey-scale variance of each block is calculated. If the variance of a block is less than the global threshold, such block is assigned to the background; otherwise, it is assigned to the foreground.[33, 34] The grey-level variance for a block of size $W \times W$ is defined as:

$$V(k) = \frac{1}{W^2} \sum_{i=0}^{W-1} \sum_{j=0}^{W-1} (I(i, j) - M(k))^2$$

(17)

$V(k)$ is the variance for block k, $I(i, j)$ is the grey-level value at pixel (i, j), and $M(k)$ is the mean grey-level value for the block k.

The segmented image is normalised for the standardization of its intensity values. Normalization is done by regulating the grey-level values to expected range. If $\rho(r, s)$ represents the grey-level value at pixel (r, s) and $\beta(r, s)$ represents the normalised grey-level value at pixel (r, s), then the normalized image is defined as:

$$\beta(r, s) = \begin{cases} \gamma_0 + \sqrt{(\vartheta_0(\rho(r, s) - \gamma)^2)\vartheta^{-1}} & if \rho(r, s) > \gamma \\ \gamma_0 - \sqrt{(\vartheta_0(\rho(r, s) - \gamma)^2)\vartheta^{-1}} & otherwise \end{cases}$$

(18)

γ and ϑ are the calculated mean and variance of $\rho(r, s)$, respectively while γ_0 and ϑ_0 are the desired mean and variance respectively.

The orientation field of a fingerprint image defines the local orientation of its ridges and it is a fundamental step in the filtering process. It is computed by dividing the image into $W \times W$ blocks and the local orientation for a block with centre at pixel (r, s) is computed from Ref.[13, 14, 35] as:

$$V_x(r,s) = \sum_{p=r-\frac{w}{2}}^{r+\frac{w}{2}} \sum_{q=s-\frac{w}{2}}^{s+\frac{w}{2}} 2\partial_x(p,q)\partial_y(p,q)$$

$$(19)$$

$$V_y(r,s) = \sum_{p=r-\frac{w}{2}}^{r+\frac{w}{2}} \sum_{q=s-\frac{w}{2}}^{s+\frac{w}{2}} \partial_x^2(p,q) - \partial_y^2(p,q)$$

$$(20)$$

$$\theta(r,s) = \frac{1}{2}\tan^{-1}\frac{V_y(r,s)}{V_x(r,s)}$$

$$(21)$$

$\partial_x(p,q)$ and $\partial_y(p,q)$ are the gradients at point (p,q) in x and y directions respectively and $\theta(r,s)$ is the least square estimate of the local orientation of the block with centre at pixel (r,s).

The ridge frequency estimation algorithm generates a coarse-level ridge map of the input fingerprint image and is based on the estimated local ridge orientations. The grey level values along fingerprint ridges and valleys are modeled as sinusoidal shaped wave along the direction normal to the local orientation. The wave is utilized for the estimation of the ridge frequency based on the assumptions that valid ridge frequencies lie between 1/31 and 1/25 for 500 dpi images.[31, 36, 37] The Gabor filter implemented in Ref.[16, 31, 32] (Equation 7) is modified based on periodic function $G(x, y : f, \theta)$ as follows:

$$G(x, y: f, \theta) = \exp\left[0.5\left[\frac{\alpha^2\vartheta_y^2 + \beta^2\vartheta_x^2}{\vartheta_x^2\vartheta_y^2}\right]\right]\cos(2\pi f\alpha)$$

$$(22)$$

$$\alpha = x\sin\theta + y\cos\theta$$

$$(23)$$

$$\beta = x\cos\theta + y\sin\theta$$

$$(24)$$

f represents the frequency of the sinusoidal plane wave along the direction θ from the x-axis, ϑ_x and ϑ_y are the space constants empirically determined and set to half of the average inter-ridge distance in their respective direction.

4. EXPERIMENTAL STUDY

The impact of different parameter values on fingerprint image filtering based on the modified Gabor filter formed the focus of the study. The experiments were conducted using the Matlab software. Fingerprint images used for the experiments were selected from the datasets of the standard FVC2002 fin-

gerprint database whose summary is presented in Table 1.[38] These datasets were selected because they contain standard and benchmarked fingerprints which were obtained from different sensors and exhibit different qualities. The experiments followed the procedure presented in Figure 3. Results of segmentation experiments on three selected images of different qualities for variance threshold below and above 100 are presented in Figure 4. Visual inspection of these results shows that for variance equals or exceeds 100, there are good segmentation results while lower variance thresholds values produced poorly segmented images (see Figures 4 (b), 4(e) and 4(g)). Overlap regions (enclosed with ovals in Figures 4(e) and 4(h)) were also noted for sub-quality (poor quality) images.

Table 1. Details of FVC2002 Fingerprint Database

Data Base	Sensor Type	Image Size KPixel	Number	Resolution
DB1	Optical	388×374 (142 Kp)	100×8	500 dpi
DB2	Optical	296×560 (162 Kp)	100×8	569 dpi
DB3	Capacitive	300×300 (88 Kp)	100×8	500 dpi
DB4	SFinGe v2.51	288×384 (108 Kp)	100×8	500 dpi

During normalization experiments, image ridge frequencies were manipulated to various values while the intensities were adjusted between 0 and 1 for different values of γ_0 and ϑ_0 and parts of the results are shown in Figure 5. For γ_0 and ϑ_0, values ranging between -1 and +1 were considered and the result presented in Figure 5(b) validates the best performance for γ_0=0 and ϑ_0=1 (which serve as optimal values) in terms of ridge contrast enhancement. For systematic determination of the optimal parameter values, experimental values were selected from the range for each parameter and the obtained results examined. Figures 6(a) and 6(c) represent the histogram plots for normalized images at γ_0=0,ϑ_0=0.5 and γ_0=0.5,ϑ_0=1, respectively. These two plots demonstrate inconsistencies in the frequencies and distributions of the intensity values along the 0 - 1 scale. The inconsistencies increase as the differences between the optimal and the actual values increases. Visual inspection of Figure 6(b) revealed that normalization at optimal parameter values γ_0=0 and ϑ_0=1 produced the best result with the ridge frequencies assuming very close values and fall within 0 and 1 scale leading to even and balanced distributions between the ridges and valleys. Objective evaluation of these parameter values based on results' computation times, consistency and accuracy proved they are most reliable and with the greatest potential for satisfactory results. An investigation of the performance of the normalization algorithm on images of diverse qualities based on these values show that for low contrast images, the Average Intensity Value (AIV) after normalization was found to be high while the reverse is the case for high contrast images.
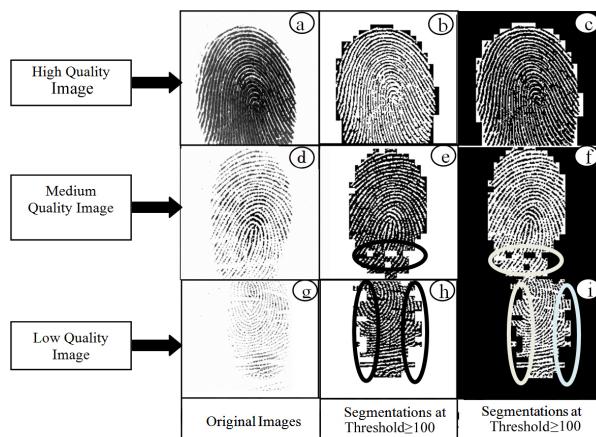
Figure 4. Results of segmentation for images of various qualities for variance threshold less or greater than 100

The AIV values for all the images in each of the four datasets of FVC2002 fingerprint database are presented in Tables 2 through 5. It is observed that images with identifier (109,6); (101,7); (102,7) and (105,5) recorded the least AIV shown in bold in Tables 2-5 respectively, while images with identifiers (104,6); (109,1); (105,5) and (107,1) recorded the highest AIV shown in bold in Tables 2-5 respectively. Visual inspec-

tion and comparison of the images and the results confirmed these results.

The most suitable block size, w for the ridge segmentation, orientation and frequency estimation experiments is 32. This value consistently gave the best results with very minimal computation time. From Equation (22), ϑ_x and ϑ_y represent standard deviation of the 2-D Gaussian function along the x and y axes respectively and they were used to control the spatial frequency bandwidth of the filter response. The higher the value of these two parameters, the higher is the expected bandwidth.
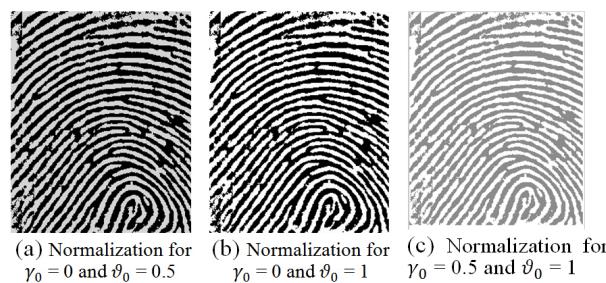

(a) Normalization for $\gamma_0 = 0$ and $\vartheta_0 = 0.5$ (b) Normalization for $\gamma_0 = 0$ and $\vartheta_0 = 1$ (c) Normalization for $\gamma_0 = 0.5$ and $\vartheta_0 = 1$

Figure 5. Results of image normalization for different parameters values
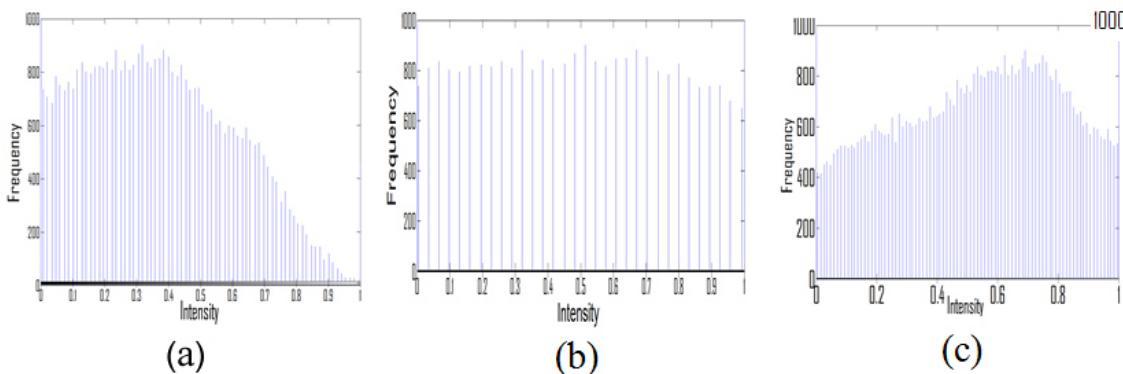
Figure 6. Histogram plot

Table 2. AIV for images in dataset DB1 of FVC 2002 Fingerprint Database

Image	Impression							
	1	2	3	4	5	6	7	8
101	0.7327	0.6697	0.7397	0.5410	0.4901	0.8360	0.8405	0.6345
102	0.7361	0.7619	0.6848	0.7256	0.5984	0.8601	0.5942	0.5855
103	0.8847	0.8290	0.8474	0.7344	0.9411	0.9225	0.8129	0.6426
104	0.7995	0.8151	0.7987	0.8545	0.7750	**0.9281**	0.9104	0.7217
105	0.7898	0.7459	0.7351	0.6636	0.7795	0.6885	0.8688	0.6288
106	0.8888	0.8761	0.9027	0.8769	0.9122	0.8634	0.8150	0.7268
107	0.7184	0.7480	0.7254	0.7397	0.7403	0.8925	0.8739	0.6021
108	0.8137	0.8127	0.7741	0.8277	0.7254	0.8699	0.8205	0.8069
109	0.5716	0.6411	0.5785	0.5353	0.5925	**0.4733**	0.7190	0.5173
110	0.6946	0.7145	0.7261	0.6759	0.6836	0.6736	0.8468	0.7189

Table 3. AIV for images in dataset DB2 of FVC 2002 Fingerprint Database

Image	Impression							
	1	2	3	4	5	6	7	8
101	0.8146	0.8574	0.8336	0.8340	0.8925	0.8880	**0.7555**	0.7807
102	0.8575	0.8691	0.8540	0.8681	0.8765	0.8453	0.8682	0.7841
103	0.8332	0.8035	0.8178	0.8042	0.7869	0.8078	0.7828	0.7687
104	0.8604	0.8581	0.8674	0.8581	0.8568	0.8649	0.8490	0.7564
105	0.8738	0.8547	0.8603	0.8376	0.8051	0.9134	0.8083	0.8009
106	0.8037	0.8255	0.8235	0.7892	0.8394	0.7900	0.8723	0.7879
107	0.7694	0.8165	0.8413	0.8394	0.7717	0.8244	0.8432	0.8676
108	0.8104	0.8213	0.7766	0.8318	0.7971	0.8343	0.8229	0.7913
109	**0.9159**	0.8748	0.8655	0.8672	0.8227	0.8361	0.8332	0.7716
110	0.8698	0.8570	0.8381	0.8083	0.8037	0.7778	0.8233	0.7972

Table 4. AIV for images in dataset DB3 of FVC 2002 Fingerprint Database

Image	Impression							
	1	2	3	4	5	6	7	8
101	0.8787	0.8880	0.8910	0.8760	0.8800	0.9005	0.7897	0.8251
102	0.8052	0.8355	0.8000	0.7967	0.9084	0.8545	**0.7216**	0.7680
103	0.8161	0.8027	0.8174	0.8725	0.9123	0.8290	0.7501	0.8042
104	0.7900	0.7748	0.7726	0.7503	0.8307	0.8272	0.8588	0.7816
105	0.8777	0.8480	0.8402	0.8956	**0.9229**	0.8814	0.7890	0.7928
106	0.8424	0.7986	0.7909	0.8562	0.6857	0.8139	0.7491	0.7628
107	0.7800	0.7653	0.7534	0.8143	0.8070	0.8034	0.7383	0.7420
108	0.7681	0.8023	0.7909	0.7994	0.9157	0.8760	0.8273	0.7907
109	0.7822	0.7567	0.7539	0.7813	0.8722	0.9061	0.7772	0.7549
110	0.8204	0.8355	0.8381	0.8589	0.8664	0.8431	0.7361	0.7716

Table 5. AIV for images in dataset DB4 of FVC 2002 Fingerprint Database

Image	Impression							
	1	2	3	4	5	6	7	8
101	0.7956	0.7911	0.7979	0.7912	0.7460	0.7731	0.7856	0.7949
102	0.8045	0.7969	0.7981	0.7874	0.7680	0.7963	0.8108	0.7932
103	0.8040	0.8051	0.8044	0.8153	0.8207	0.8002	0.8085	0.7835
104	0.8098	0.8065	0.7912	0.7625	0.7888	0.7592	0.7715	0.7716
105	0.7527	0.7527	0.7692	0.7767	**0.7391**	**0.7391**	0.7896	0.7733
106	0.7835	0.7441	0.7615	0.7955	0.7824	0.8019	0.7495	0.7415
107	**0.8345**	0.8126	0.8016	0.8053	0.7840	0.8204	0.7769	0.8169
108	0.7785	0.8059	0.8000	0.7903	0.8142	0.7970	0.7647	0.7927
109	0.8004	0.8047	0.7821	0.7992	0.7795	0.7878	0.8134	0.7880
110	0.8100	0.8199	0.8145	0.7998	0.8133	0.8034	0.7861	0.7762

When the bandwidth is too high, noises can be unnecessarily magnified while too low bandwidth hampers some useful signals.[15] ϑ_x greatly influences the degree of contrast enhancement between ridges and valleys and its values were carefully specified. The specifications involve trade-off between accuracy and speed. With exceedingly large ϑ_x, there were enhancement artifacts and significant amount of blurring of the ridge structures while too small ϑ_x results in ineffective removal of noise and a mere smoothening of the original image. The value of ϑ_y dictates the extent to which filtering is done along the local orientation with too large value resulting in the blurring of some minutiae. For fingerprint image filtering, the authors in Ref.[15,31] empirically set values of ϑ_x and ϑ_y to 4.0 while they were specified to 3.0 and 4.0 respectively in Ref.[15] In the current study, ϑ_x and ϑ_y were empirically specified to 5.0 and experimental studies of the different algorithms and their parameter values were carried out based on selected images from FVC2002 fingerprint datasets. Filtered results based on parameters specified in the current study are presented in Figure 7 while Figure 8 shows the filtering results based on Gabor filter algorithms and values specified in Ref.[15,25,31]

The filtering results for the current study presented in Figures 7(d), 7(e) and 7(f) show best performances in term of clarity of the ridges and orientation smoothening. Visual inspection of Figure 8 reveals several loss of connection among ridges which is attributed to insufficient filtering of the images.

For a further proof of the superiority of the modified algo-

rithm and its set parameters over some of the existing ones, skeletons of the filtered images were obtained by passing them as inputs to the MATLAB's *bwmorph* operation using "*thin*" option. In a skeleton image, all forms of ridge overlap are removed resulting in clear separation between the ridges and valleys. The connectivity of the ridge structures are preserved while the ridge thickness is reduced to one pixel wide. Some popular fingerprint filtering algorithms are presented by the authors in Ref.[15,25,31]
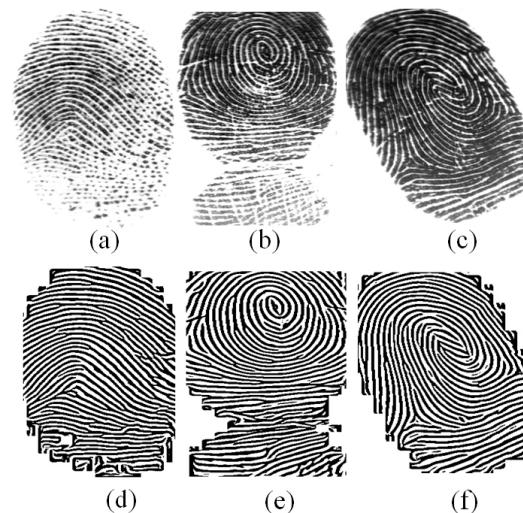

(a)   (b)   (c)

(d)   (e)   (f)

Figure 7. Filtered images of selected fingerprints based on specified parameters

(a)   (b)   (c)

(ϑ_x= 0.4, ϑ_y= 0.4)

(d)   (e)   (f)

(ϑ_x= 0.3, ϑ_y= 0.4)

Figure 8. Filtered images of selected fingerprints based on parameters specified in Ref.[15,25,31]

They exhibit similar parameters and characteristics with the one presented in the current study and these motivated their choice for comparative study. The results for the filtered images presented in Figures 7 and 8 are shown in Figure 9. Figures 9(a-c) were produced by the modified Gabor filter algorithm at ϑ_x=0.5, ϑ_y=0.5 while Figures 9(d-f) and Figures 9(g-i) were the results obtained for algorithms and parameters presented in Ref.[15,25,31] respectively. Visual inspection of Figure 9 indicates best result in term of ridge connectivity and preservation for the modified algorithm.
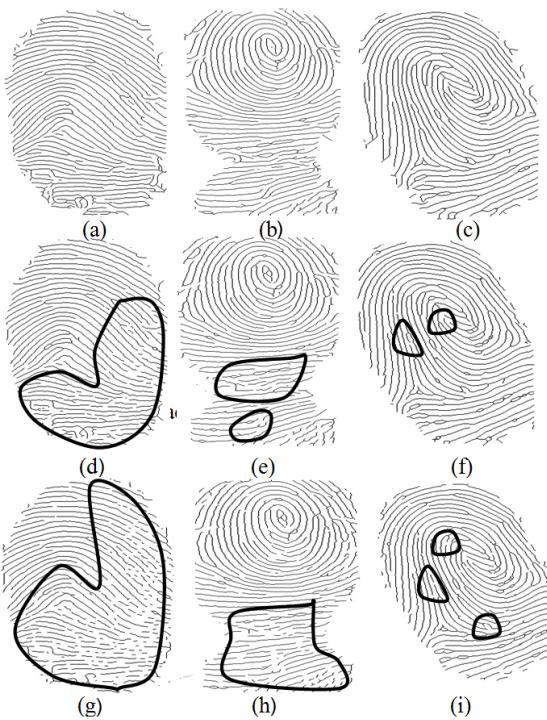

Figure 9. Skeleton images for different algorithms and parameter

It is also revealed that the skeletons presented in Figures 9(d-i) contain missing connections among ridges (some of which are enclosed in circles) which is attributed to tuning failure on the part of the algorithms and their associated parameter values. The suitability of each algorithm and its parameter values as a platform for reliable and satisfactory detection and extraction of minutiae points for AFIS-based systems was also investigated. A fingerprint minutiae set is a composition of all its extracted minutiae and it is an essential component whose characteristics form the basis for verification and identification exercise in AFIS. The algorithm presented in Ref.[39] is implemented for the detection and extraction of minutiae from a fingerprint image. Minutiae points extracted from the skeletons of the filtered images obtained from the current algorithm and its set parameters

are presented in Figure 10 (a-c). Figures 10(d-f) and 10(g-i) show extracted points from the skeletons of filtered images obtained via Ref.[15,31] and Ref.[25]-based algorithms and parameter values, respectively.
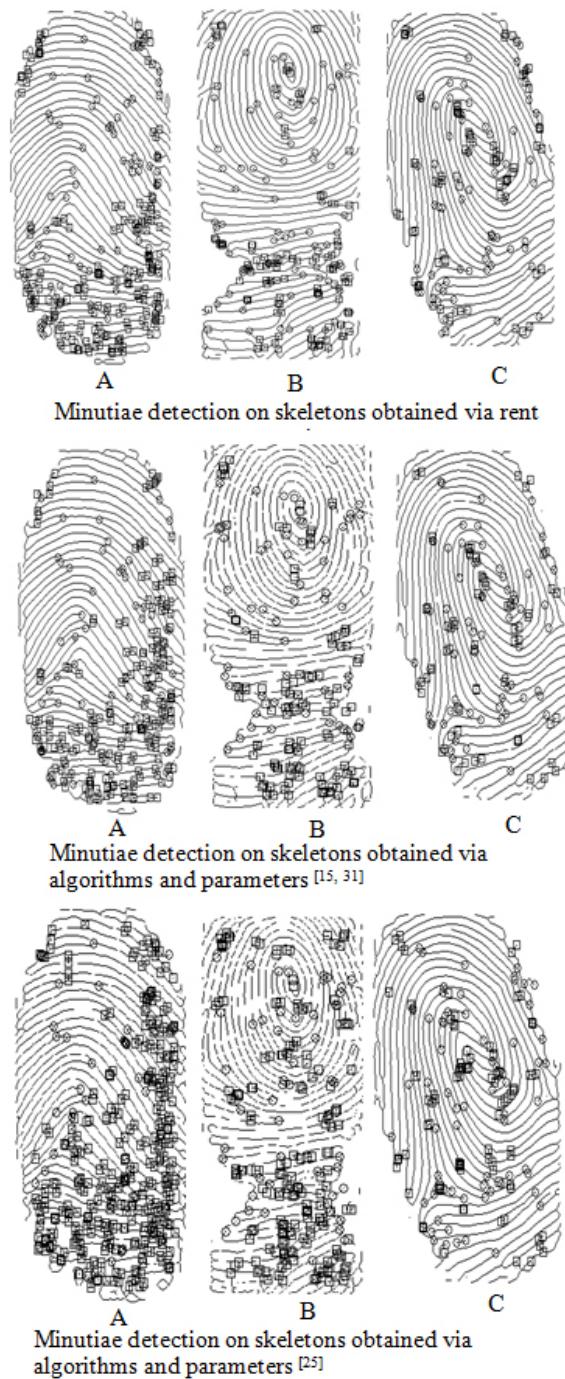

Figure 10. Minutiae detection on skeletons obtained via current study

The valid minutiae points are shown in circles and represent the genuine points at which the ridge terminates or bifurcates while the false minutiae points are the points with connection

failures or created as artifacts[39] and they are presented in square boxes. Table 6 presents the statistics of the detected true and false minutiae points in the three images by the three algorithms and their associated parameter values. In all cases, the skeleton of the filtered images obtained using the modified algorithm and its parameters recorded the highest number of true minutiae and the lowest number of false minutiae points.

The cumulative true and false minutiae detections for all fingerprints in the four datasets of FVC2002 fingerprint database based on the three sets of algorithms and parameter

values are also presented in Table 7. The results equally indicate highest number of valid points (as well as least number of false points) for the images obtained via the modified algorithm and its parameter values. The generation of fewest numbers of false minutiae points on the images produced via the modified Gabor filter and its parameters values confirms its superiority. In practical applications, the new algorithm and its parameter values will reduce the tasks and times associated with the elimination of false minutiae points (which have been reported to exert negative impact on the speed and accuracy of AFIS[40]). In other words, the new algorithm will promote speedy and more efficient AFIS.

Table 6. Statistics of detected true and false minutiae points in three images (A = image shown in Figure 7(a), B = image shown in Figure 7(b), C = image shown in Figure 7(c))

Image	True			False		
	Ref. [25]	Ref. [15,31]	Current Study	Ref. [25]	Ref. [15,31]	Current Study
A	30	53	69	374	201	177
B	51	54	74	176	112	105
C	61	55	64	91	80	74

Table 7. Cumulative true and false minutiae point detections for FVC2002 fingerprints

Dataset	True			False		
	Ref. [25]	Ref. [15,31]	Current Study	Ref. [25]	Ref. [15,31]	Current Study
DB1	4,234	5,157	6,453	12,489	7,437	8,179
DB2	8,225	9,660	10,346	22,537	16,277	15,979
DB3	4,957	7,845	8,042	25,017	14,682	11,996
DB4	6,339	8,762	9,314	30,783	17,361	15,010

5. CONCLUSION

An experimental study of the impact of a modified Gabor filter and its parameter values on fingerprint filtering has been reported. The existing Gabor filter was modified purposely for improvement based on selected periodic functions and optimal parameter values. For the purpose of obtaining stable and reliable fingerprint filtering results, pre-processing stages of segmentation, normalization, ridge orientation and frequency estimations were considered as important. Obtained results from comparison with other Gabor filter algorithms and parameter values showed superior fingerprint

image filtering. Due to its improved capability, the algorithm is able to filter out false minutiae points and extract only true minutiae points thereby making it suitable for implementing AFIS with greater response time, which ultimately place it at vantage position over some existing algorithms. The main challenge to the study is the failure in cases of severely corrupted regions of fingerprint image. When this occurs, one or more of the pre-processing stages may fail and consequently, lead to difficulty in obtaining accurate and adequate result. Future research therefore focuses on suppressing corrupted regions for minimal effect on filtering.

REFERENCES

[1] Roberts. Biometrics. Accessed: July, 2009. Available from: `http://www.ccip.govt.nz/newsroom/informoation-not es/2005/biometrics.pdf`

[2] Liu W. Fingerprint Classification Using Singularities Detection. Inter-

national Journal of Science and Research (IJSR). 2013; 2(1): 158-62.

[3] Kaur JN, Kamra A. A Novel Method for Fingerprint Core Point Detection. International Journal of Scientific and Engineering Research. 2011; 2(4): 1-6.

[4] Jin B, Ping TH, Lan XM. Fingerprint Singular Point Detection Algo-

rithm by Poincaré Index. WSEAS Transactions on Systems. 2008; 7(12): 1453-62.

[5] Iwasokun GB, Akinyokun OC, Olabode O. A Mathematical Modeling Approach to Fingerprint Ridge Segmentation and Normalization. International Journal of Computer Science. Information Technology and Security, Singapore. 2012; 2(2): 263-7.

[6] Iwasokun GB, Akinyokun OC, Angaye CO. Fingerprint Matching using Neighborhood Distinctiveness. International Journal of Computer Applications. 2013; 66(21): 1-8.

[7] Mukerji M. DSP Implementation of a Fingerprints-based Biometric Authentication System. Part 4 Final Project Report, Department of Electrical and Computer Engineering, University of Auckland, New Zealand; 2004. p. 7-12.

[8] Nanavati S, Thieme M, Nanavati R. Biometrics, Identifying Verification in a Networked World, John Wiley & Sons, Inc.; 2002. p. 15-40.

[9] Sara N, Sergie D, Gregory V. User Interface Design of the Interactive Fingerprint Recognition (INFIR) System. Unpublished, 2004: 1-8. Accessed 16/05/2014. `http://citeseerx.ist.psu.edu/view doc/download?doi=10.1.1.86.4209&rep=rep1&type=pdf`

[10] Setlak DR. Advances in Fingerprint Sensors using RF Imaging Techniques. Automatic Fingerprint Recognition Systems. 2004; 8(3): 27-53. `http://dx.doi.org/10.1007/0-387-21685-5_2`

[11] Ratha NK, Karu K, Chen S, et al. A Real Time Matching System for Large Fingerprint Databases. IEEE Transactions on Pattern Analysis and Machine Intelligence. 2004; 16(8): 800-13.

[12] Iwasokun GB. Development of a Hybrid Platform for the Pattern Recognition and Matching of Thumbprints, Unpublished PhD Thesis, Department of Computer Science, Federal University of Technology, Akure, Nigeria. 2012.

[13] Raymond T. Fingerprint Image Enhancement and Minutiae Extraction. Unpublished PhD Thesis, School of Computer Science and Software Engineering, University of Western Australia. 2003. Accessed 12/04/2008. `www.peterkovesi.com/studentprojects/ raymondthai/RaymondThai.pdf`

[14] Liu H, Yifei W, Jaiu A. Fingerprint Image Enhancement: Algorithm and Performance Evaluation. Pattern Recognition and Image Processing Laboratory, Department of Computer Science, Michigan State University. 2006. Accessed 09/08/2013(`www.math.tau.ac.il/~t urkel/imagepapers/fingerprint.pdf`).

[15] Jianwei Y, Lui L, Jiang T, et al. A Modified Gabor Filter Design Method for Fingerprint Image Enhancement. Pattern Recognition Letters. 2003; 24: 1805-17. `http://dx.doi.org/10.1016/S01 67-8655(03)00005-9`

[16] Hongchang K, Hui W, Degang K. An Improved Gabor Filtering for Fingerprint Image Enhancement Technology. Proceedings of the Second International Conference on Electronic and Mechanical Engineering and Information Technology, France, Atlantis Press; 2012. p. 1238-41.

[17] Dhanabal R, Bharathi V, Jain GP, et al. Gabor Filter Design for Fingerprint Application Using Matlab and Verilog HDL. International Journal of Engineering and Technology (IJET). 2013; 5(2): 1386-91.

[18] Sharat C, Cartwright AN, Govindaraju V. Fingerprint Image Enhancement Using STFT Analysis. Pattern Recognition. 2007; 40: 198–211. `http://dx.doi.org/10.1016/j.patcog.2006.05.036`

[19] Prajakta MM, Ramesh PA. A Novel Approach to Fingerprint Identification Using Gabor Filter-Bank. ACEEE International Journal on Network Security. 2011; 2(3): 10-4.

[20] Sherlock BG, Monro DM, Millard K. Fingerprint Enhancement by Directional Fourier Filtering. Proceedings of IEEE on Vision Image Signal Process. 1994; 141(2): 87-94. `http://dx.doi.org/10.10 49/ip-vis:19949924`

[21] Aarthy V, Mythili R, Mahendran M. Low Quality Fingerprint Image Using Spatial and Frequency Domain Filter. International Journal of Computational Engineering Research. 2012; 2(6): 80-3.

[22] Josef SB, Mikael N, Jorgen N, et al. Adaptive Fingerprint Binarization by Frequency Domain Analysis. Proceedings of Fortieth Asilomar Conference on Signals, Systems and Computers, Pacific Grove, CA; 2006. p. 598-602.

[23] Pannirselvam S, Raajan P. An Efficient Finger Print Enhancement Filtering Technique with High Boost Gaussian Filter (HBG). International Journal of Advanced Research in Computer Science and Software Engineering. 2012; 2(11): 370-8.

[24] Yigang Z, Yuhua J, Juncao L, et al. A Fingerprint Enhancement Algorithm using Federated Filter. 2014: 1-5. Unpublished. Accessed 25/05/2014, `http://web.cecs.pdx.edu/~juncao/links/my papers/A%20Fingerprint%20Enhancement%20Algorithm%2 0using%20a%20Federated%20Filter.pdf`

[25] Greenberg S, Aladjem M, Kogan Dand Dimitrov I. Fingerprint Image Enhancement using Filtering Techniques. Real-Time Imaging. 2002; 8: 227-36. `http://dx.doi.org/10.1006/rtim.2001.0283`

[26] Amjad A, Xiaojun J, Jie Z, et al. Fingerprint Image Enhancement Using Coherence Diffusion Filter and Gabor Filter. Journal of Information and Computational Science. 2012; 9(1): 153-160.

[27] Gualberto A, Gabriel S, Karina T, et al. Automatic Fingerprint Recognition System Using Fast Fourier Transform and Gabor Filters. Científica. 2008; 12(1): 9-16.

[28] Gabor D. Theory of Communication. Journal of IEEE. 1946; 93: 429-57.

[29] Daugman JG. Two-dimensional Spectral Analysis of Cortical Receptive Field Profiles. Journal of Vision Research. 1980; 20: 847-56. `http://dx.doi.org/10.1016/0042-6989(80)90065-6`

[30] Daugman JG. Uncertainty Relation for Resolution in Space, Spatial Frequency, and Orientation Optimized by Two-Dimensional Visual Cortical Filters. Journal of Optical Society. USA. 1985; 2(7): 1160-9. `http://dx.doi.org/10.1364/JOSAA.2.001160`

[31] Hong L, Wan Yand Jain A. Fingerprint Image Enhancement: Algorithm and Performance Evaluation. IEEE Transactions on Pattern Analysis and Machine Intelligence. 1998; 20: 777-89. `http: //dx.doi.org/10.1109/34.709565`

[32] Jain AK, Farrokhnia F. Unsupervised Texture Segmentation using Gabor Filters. Journal of Pattern Recognition. 1991; 24(12): 1167-86. `http://dx.doi.org/10.1016/0031-3203(91)90143-S`

[33] Iwasokun GB, Akinyokun OC, Alese BK, et al. A Multi-Level Model for Fingerprint Enhancement. Lecture Notes in Engineering and Computer Science: Proceedings of The International Multi-Conference of Engineers and Computer Scientists. IMECS 2012. 14-16 March, 2012, Hong Kong, Pages 730-735. Available from: `www.iaeng.org/publication/IMECS2012`

[34] Iwasokun GB, Akinyokun OC, Angaye CO, et al. A Multi-Level Model for Fingerprint Enhancement. Journal of Pattern Research, USA. 2012; 7: 155-74. `http://dx.doi.org/10.13176/11.352`

[35] Iwasokun GB, Akinyokun OC, Olabode O. A Block Processing Approach to Fingerprint Ridge Orientation Estimation. Journal of Computer Technology and Application, USA. 2012; 3: 401-7.

[36] Arun VC. Extracting and Enhancing the Core Area in Fingerprint Images. IJCSNS International Journal of Computer Science and Network Security. 2007; 7(11): 16-20.

[37] Iwasokun GB, Akinyokun OC, Olabode O. Uniformity Level Approach to Fingerprint Ridge Frequency Estimation. International Journal of Computer Applications. 2013; 61(22): 26-32.

[38] Cappelli R, Maio D, Maltoni D, et al. Performance Evaluation of Fingerprint Verification Systems. IEEE Transactions on Pattern Anal-

ysis and Machine Intelligence. 2006; 28(1): 3-18. PMid:16402615. http://dx.doi.org/10.1109/TPAMI.2006.20

[39] Iwasokun GB, Akinyokun OC, Alese BK, *et al*. Adaptive and Faster Approach to Fingerprint Minutiae Extraction and Validation. International Journal of Computer Science and Security (IJCSS). 2011; 5(4): 414-24.

[40] Iwasokun GB, Akinyokun OC, Ojo SO. An Investigation into the Impact of False Minutiae Points on Fingerprint Matching. International Journal of Database Theory and Application. 2014; 7(3): 159-78. http://dx.doi.org/10.14257/ijdta.2014.7.3.15